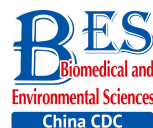


Original Article



Role of Endoplasmic Reticulum Stress in Silica-induced Apoptosis in RAW264.7 Cells*

HU Yong Bin^{1,2,&}, WU Xia^{1,3,&}, QIN Xiao Feng¹, WANG Lei², and PAN Pin Hua^{4,#}

1. Department of Pathology, Xiangya Basic Medical School, Central South University, Changsha 410013, Hunan, China; 2. Department of Pathology, Xiangya Hospital, Central South University, Changsha 410008, Hunan, China; 3. Department of Pathology, The Second Xiangya Hospital, Central South University, Changsha 410011, Hunan, China; 4. Department of Respiratory Medicine, Xiangya Hospital, Central South University, Changsha 410008, Hunan, China

Abstract

Objective We investigated the role of endoplasmic reticulum stress (ERS) in silica-induced apoptosis in alveolar macrophages *in vitro*.

Methods RAW264.7 cells were incubated with 200 µg/mL silica for different time periods. Cell viability was assayed by the MTT assay. Cell apoptosis was evaluated by DAPI staining, flow cytometry analysis, and Western blot analysis of caspase-3. Morphological changes in the endoplasmic reticulum were observed by transmission electron microscopy. The expression of ERS markers binding protein (BiP) and CCAAT-enhancer-binding protein homologous protein (CHOP) was examined by Western blotting and real-time PCR. As an inhibitor of ERS, 4-phenylbutyric acid (4-PBA) was used in the experiments.

Results Silica exposure induced nuclear condensation and caspase-3 expression in RAW264.7 cells. The number of apoptotic cells increased after silica exposure in a time-dependent manner. Silica treatment induced expansion of the endoplasmic reticulum. In addition, the expression of BiP and CHOP increased in silica-stimulated cells. Furthermore, 4-PBA treatment inhibited silica-induced endoplasmic reticulum expansion and the expression of BiP and CHOP. Moreover, 4-PBA treatment attenuated nuclear condensation, reduced apoptotic cells, and downregulated caspase-3 expression in silica-stimulated cells.

Conclusion Silica-induced ERS is involved in the apoptosis of alveolar macrophages.

Key words: Silica; Alveolar macrophages; Endoplasmic reticulum stress; Apoptosis

Biomed Environ Sci, 2017; 30(8): 591-600

doi: 10.3967/bes2017.078

ISSN: 0895-3988

www.besjournal.com (full text)

CN: 11-2816/Q

Copyright ©2017 by China CDC

INTRODUCTION

Inhalation of silica particles can result in the development of an inflammatory response and fibrosis in the lungs. Alveolar macrophages (AM) are the main target cells of silica

dust. AM normally play a protective role in the lungs by clearing foreign materials^[1-2]. Silica induction leads to macrophage activation and phagocytosis, as well as the production of proinflammatory cytokines. Many studies have indicated that silica-induced activation of macrophages is associated with

*This work was supported by the National Natural Science Foundation of China (No 81673120); China Postdoctoral Science Foundation (2014M562139); and Hunan Province Natural Science Foundation (14JJ2041).

&These authors contributed equally to this work.

#Correspondence should be addressed to Professor PAN Pin Hua, Tel/Fax: 86-731-89753287, E-mail: Pinhuapan668@126.com

Biographical notes of the first authors: HU Yong Bin, born in 1977, male, Associate Professor and PhD, majoring in pulmonary pathology; WU Xia, born in 1988, MD, female, majoring in pulmonary pathology.

autophagy^[3-4]. Silica exposure was shown to enhance autophagic activity in bone marrow-derived macrophages *in vitro* and in AM isolated from silica-exposed mice *in vivo*^[5]. Autophagy, an alternative cell death pathway, is closely linked with apoptosis. Silica phagocytosis also causes apoptosis in AM^[6-7]. There is substantial evidence that apoptosis of macrophages that take up silica particles plays a significant role in the etiology of silicosis^[8-9]. AM apoptosis itself is an important event in silicosis and is associated with innate immune cell infiltration and increased collagen deposition^[10]. However, the underlying regulation mechanism of silica-induced apoptosis remains unclear.

The endoplasmic reticulum (ER) is an intracellular organelle in which secretory and membrane proteins are assembled. The ER is also responsible for the quality control of protein folding and intracellular calcium homeostasis. Errors in protein folding in the ER lumen can lead to accumulation of endoplasmic reticulum stress (ERS), which has been traditionally viewed as an adaptive mechanism and is also known as the unfolded protein response (UPR)^[11]. Activation of the UPR pathway requires the activation of three sensor proteins: inositol-requiring enzyme 1 (IRE-1), activating transcription factor 6 (ATF6), and protein kinase RNA-like ER kinase (PERK)^[12]. The UPR aims to remove the accumulated protein misfolding load, thus preventing further ERS. Prolonged ERS may activate downstream PERK-eukaryotic initiation factor 2/activating transcription factor 4/the CCAAT-enhancer-binding protein homologous protein (CHOP)-dependent pathway, which eventually cleaves caspase-3 to mediate cell apoptosis^[13-15]. Although numerous situations can lead to protein misfolding in the ER, such as ischemia reperfusion injury, oxidative stress, calcium metabolism disorder, or simply increased secretory protein synthesis^[16-18], silica-induced ERS in AM apoptosis is not well-understood.

In this study, we treated RAW264.7 cells with silica and explored the induction of apoptosis and ERS. Whether ERS mediates silica-induced apoptosis was determined.

MATERIALS AND METHODS

Preparation of Crystalline Silica

Crystalline silica (Sigma, St. Louis, MO, USA, 0.1-10 μm in diameter) was prepared by washing

with HCl to remove contaminating Fe_2O_3 . Briefly, silica was boiled in 1 mol/L HCL, washed, and dried in an oven at 110 °C for 90 min. The particles were sterilized by heating at 180 °C for 6 h^[19]. Before use, the particles were suspended in 1 mL of sterile saline and sonicated for 10 min.

Cell Culture

RAW264.7 (American Type Culture Collection, Manassas, VA, USA) cells were maintained in high-glucose DMEM (Gibco, Grand Island, NY, USA) containing 10%-12% fetal bovine serum, penicillin (1000 IU/mL), and streptomycin (1000 IU/mL) overnight at 37 °C with 5% CO_2 . The cells were cultured in a 100-mL culture bottle until 60%-80% confluence, and then placed in dulbecco's modified eagle medium (DMEM) containing only 0.5% fetal bovine serum for 24 h before induction. Silica was prepared as 200 $\mu\text{g/mL}$ samples in DMEM, and added to the cells.

Reagents

Tunicamycin (Sigma), a reagent that strongly induces ERS by disrupting *N*-linked protein glycosylation^[5], was prepared as a concentrated stock solution (10 mg/mL) in dimethyl sulfoxide. 4-Phenylbutyric acid (4-PBA, Sigma) was dissolved in DMEM at a concentration of 1000 mmol/L and diluted to the desired concentration directly in culture medium.

MTT Assay

Cell viability was assayed using the MTT test. The cells were exposed to silica (200 $\mu\text{g/mL}$) for 0, 6, 12, 24, and 48 h. At the end of the experimental period, MTT (5 mg/mL) was added to the wells (20 $\mu\text{L/well}$). After 4-h incubation at 37 °C, the media were removed and dimethyl sulfoxide was added (150 $\mu\text{L/well}$). The plates were shaken at room temperature for 10 min. The absorbance value of every well at a wavelength of 570 nm was quantified using an enzyme-linked immunosorbent assay reader. Viable cells produced a dark blue formazan product, whereas no such staining occurred in dead cells.

Transmission Electron Microscopy

The cells were incubated with silica (200 $\mu\text{g/mL}$) for the indicated periods. Next, the cells were fixed with 2% formaldehyde and 2.5% glutaraldehyde in 100 mmol/L phosphate buffer solution. Post-fixation was conducted with 1.0% osmium tetroxide in

cacodylate buffer (pH 7.2), 0.8% potassium ferricyanide, and 5 mmol/L CaCl₂, and then the cells were washed in 0.1 mol/L cacodylate buffer (pH 7.2). The cells were dehydrated in an acetone series and embedded in Spurr's resin. Thin sections (60-70 nm) were collected on 300 mesh copper grids, counterstained with uranyl acetate and lead citrate, and finally observed with an H500 Transmission Electron Microscope (Hitachi, Tokyo, Japan).

Real-time PCR

Briefly, total cellular RNA was prepared using Trizol reagent according to the manufacturer instructions (TaKaRa, Shiga, Japan). Total RNA was reverse-transcribed into cDNA using a random primer (TaKaRa). The forward primer for PCR amplification of BiP mRNA was 5'-GAACACTG TGGTACCCACCAAGAA-3' and the reverse primer was 5'-TCCAGTCAGATCAAATGTACCCAGA-3'. The forward primer of CHOP was 5'-AATAACAGCCGGAACC TGAGGA-3' and the reverse primer was 5'-ACTCAG CTGCCATGACTGCAC-3'. For real-time PCR analysis, the reaction mixture containing cDNA template, primers, and SYBR Green premix (TaKaRa) was amplified in the ABI 7500 Fast Real-time PCR System (Applied Biosystems, Foster City, CA, USA). Fold-changes in mRNA levels were determined after normalization to the RNA levels of the internal control, β -actin.

Western Blot Analysis

The cells were incubated with silica (200 μ g/mL) for different times. After treatment for the indicated times, the cells were harvested and total protein was extracted. Equal amounts of cell proteins, quantified with a BCA protein assay kit (Pierce Biotechnology, Rockford, IL, USA) were resolved by 10% SDS-PAGE and transferred to nitrocellulose membranes. The membranes were blocked with 5% nonfat milk for 2 h and then incubated with various antibodies for 18 h at room temperature. After incubation with the secondary antibody at room temperature for 2 h, immunoreactive bands were visualized by enhanced chemiluminescence reactions. The rabbit polyclonal anti-GRP78/BiP, anti-CHOP, and anti-caspase-3 antibodies were obtained from Cell Signaling (Danvers, MA, USA), and anti- β -actin was from Proteintech (USA).

DAPI Staining

4,6-Diamidino-2-phenylindole (DAPI, KeyGEN

Biotech, Nanjing, China), a DNA-specific dye, was used to detect apoptosis. Cultured cells were mixed with 500 μ L DAPI for 30 min at room temperature. The excitation wavelength was 340 nm and emission fluorescence was detected with a 380-nm filter. Morphological changes of the cells were observed under the a fluorescence microscope (Olympus, Tokyo, Japan).

Flow Cytometry Analysis

Analysis of apoptosis was performed with a Annexin-V-FITC Apoptosis Detection Kit (Invitrogen, Carlsbad, CA, USA). Samples from different groups were collected by trypsinization and washed twice with cold phosphate-buffered saline. Analyses were performed on a Cytomics FC500 (Beckman Coulter, Brea, CA, USA). Cells were resuspended in 400 μ L Annexin-V binding buffer, mixed with 5 μ L Annexin-V-FITC, incubated at 2-8 $^{\circ}$ C for 15 min, and then mixed with 10 μ L propidium iodide followed by incubation at 2-8 $^{\circ}$ C for 5 min in the dark.

Statistics Analysis

All experiments were performed at least three times. A *P* value < 0.05 was considered to indicate statistical significance and determined by one-way analysis of variance. Data are presented as the mean \pm standard deviation.

RESULTS

Silica Treatment Decreases Cell Viability of RAW264.7 Cells

To detect the effects of silica on the cell viability of RAW264.7 cells, the cells were incubated with silica (200 μ g/mL) for 0, 6, 12, 24, and 48 h. After incubation, cell viability was evaluated using an MTT assay. The absorbance values derived from control or silica-exposed cells were compared. As shown in Table 1, silica decreased cell viability.

Table 1. Effect of Silica (200 μ g/mL) on Cell Viability of RAW264.7 Cells

Time/OD Value (h)	Control	200 μ g/mL Silica Group
0	0.265 \pm 0.041	0.265 \pm 0.041
6	0.467 \pm 0.050	0.275 \pm 0.013*
12	0.594 \pm 0.027	0.343 \pm 0.032*
24	0.676 \pm 0.016	0.431 \pm 0.033*
48	0.865 \pm 0.015	0.582 \pm 0.029*

Note. *: *P* < 0.05, compared with control.

Silica Treatment Induces Apoptosis of RAW264.7 Cells

To investigate the effect of silica on the apoptosis of RAW264.7 cells, we detected apoptotic cells by fluorescent microscopy after DAPI staining. Silica induced prominent nuclear changes in treated cells (Figure 1). The nuclei were round, intact, and uniformly stained in control cells. However, at 24

and 48 h, silica exposure induced nuclear condensation, resulting in smaller nuclei that displayed membrane blebbing and fragmentation as the cells died. Nuclear changes were not significant at 6 and 12 h (data not shown). Next, to quantify silica-induced apoptosis, we performed flow cytometry. As shown in Figure 2, apoptotic cells were increased time-dependently by silica exposure.

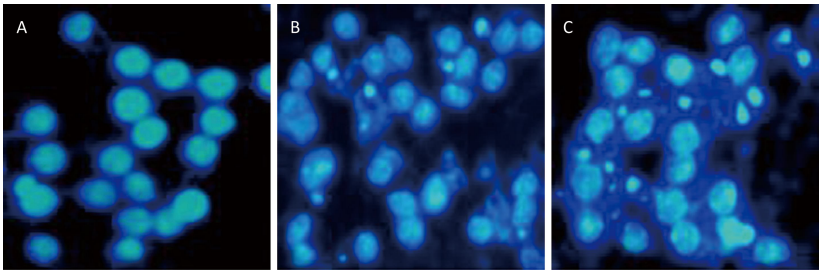


Figure 1. Silica treatment induced nuclear changes in RAW264.7 cells. Cells were treated with silica (200 $\mu\text{g/mL}$) for 0 h (A), 24 h (B), and 48 h (C) (magnification $\times 400$). Morphological changes of cells nuclei were observed by DAPI staining under a fluorescence microscope.

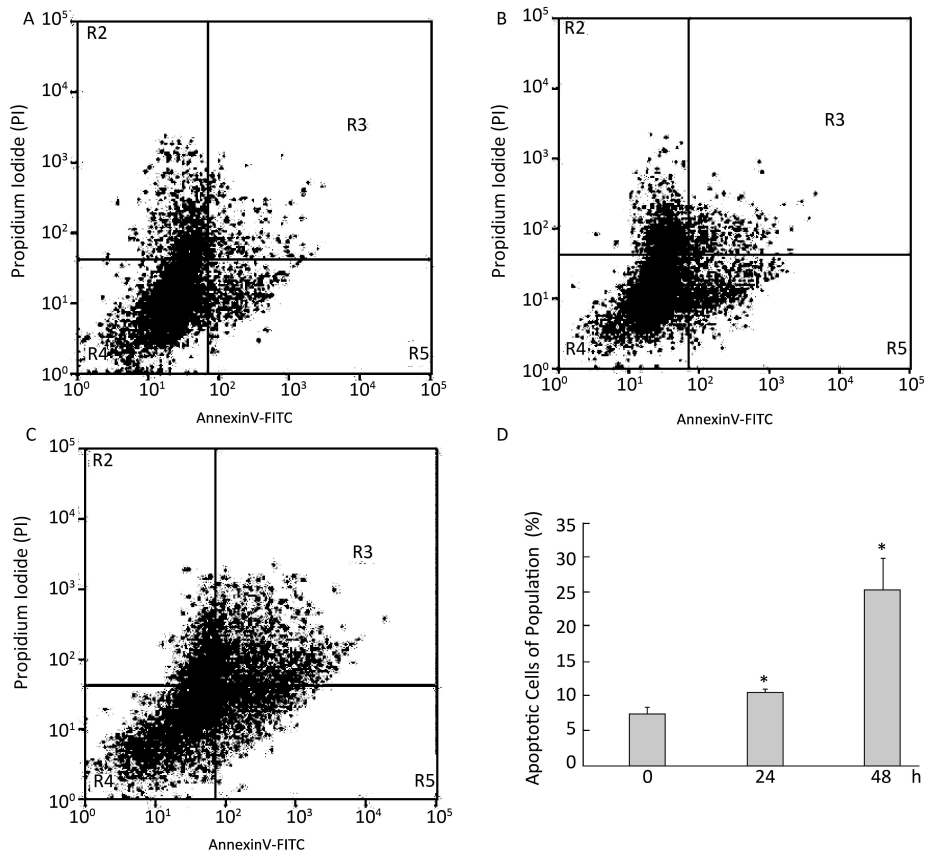


Figure 2. Silica treatment induced apoptosis of RAW264.7 cells. Cells were treated with silica (200 $\mu\text{g/mL}$) for 0 h (A), 24 h (B), and 48 h (C). Apoptotic cells were observed by flow cytometry. All histograms show apoptotic cell populations (%) (D). *: $P < 0.05$, compared with 0 h group.

Furthermore, the level of cleaved caspase-3, which induces apoptosis, was detected in silica-treated cells. The expression of caspase-3 increased at 24 h and peaked at 48 h after silica exposure (Figure 3).

Silica Treatment Induces Endoplasmic Reticulum Expansion in RAW264.7 Cells

We performed transmission electron microscopy to observe the endoplasmic reticulum of silica-induced RAW264.7 cells. ER expansion was observed at 6 h after silica treatment and the extent of ER expansion increased gradually in a time-dependent manner in silica-treated cells (Figure 4).

Silica Treatment Induces ERS in RAW264.7 Cells

To determine the effect of silica on ERS, we examined the expression of ER stress markers GRP78/BiP and CHOP. As shown in Figure 5, silica caused a notable increase in the expression of BiP mRNA and protein. Maximum induction was observed at 6 h. Additionally, silica induced CHOP expression, which was increased in a time-dependent manner (Figure 5).

4-PBA Inhibits Silica-induced Endoplasmic Reticulum Expansion of RAW264.7 Cells

To identify the role of ERS in silica-induced apoptosis in RAW264.7 cells, we selected 4-PBA as an ERS inhibitor. First, we detected the effect of 4-PBA on endoplasmic reticulum expansion. The results showed that 4-PBA inhibited silica-induced endoplasmic reticulum expansion (Figure 6).

4-PBA Inhibits Silica-induced Endoplasmic Reticulum Stress of RAW264.7 Cells

Next, we examined the effect of 4-PBA on the expression of ER stress markers BiP and CHOP in silica-stimulated cells. The results showed that 4-PBA (1, 10, 20 $\mu\text{mol/L}$) inhibited silica-induced mRNA and protein expression of BiP (Figure 7). In addition, pretreatment with 4-PBA (10, 20 $\mu\text{mol/L}$) decreased the mRNA and protein expression of CHOP (Figure 7).

4-PBA Inhibits Silica-induced Apoptosis of RAW264.7 Cells

Next, we investigated the effect of 4-PBA on apoptosis induction by silica. DAPI staining showed that pretreatment with 4-PBA attenuated nuclear condensation in silica-stimulated cells (Figure 8). In addition, flow cytometry analysis demonstrated that 4-PBA prevented silica-induced apoptosis of

RAW264.7 cells (Figure 9). The expression of cleaved caspase-3 was also decreased by 4-PBA in silica-treated cells (Figure 10).

DISCUSSION

Silicosis is a progressive, disabling, and fatal disease that eventually causes pulmonary fibrosis. Once silicon particles arrive inside the alveoli, they are taken up by AM, which play an important role in the recognition, uptake, and clearance of particles from the lung^[20]. Phagocytosis of silica results in phagosome formation, lysosomal membrane permeabilization, and release of cathepsins into the cytosol, contributing to inflammasome activation and apoptosis signaling^[21-22]. RAW264.7 cells, derived from a mouse peritoneal macrophage cell line, have the same characteristics as AM^[23]. In the present study, silica induced the apoptosis of RAW264.7 cells. The results agree with those of previous reports^[2,8]. However, the specific mechanisms of silica-induced apoptosis have not been elucidated.

ER is the major site of protein synthesis, protein folding, and secretion as well as calcium storage, which are required for normal cellular function. Recent studies suggested that ERS pathways mediate apoptosis in lung diseases induced by particles and pathogens^[24-25]. Therefore, we evaluated the influence of silica on ERS in RAW264.7 cells. Electron microscopy analysis revealed a massive expansion of the ER in RAW264.7 cells after silica treatment.

Next, we examined the marker molecules of ERS in silica-treated RAW264.7 cells. Any changes in homeostasis of the ER can activate a conserved signal transduction pathway, known as the UPR or ERS response. IRE1, PERK, and ATF6 are the three transmembrane proteins that transmit the unfolded protein signal across the ER. BiP and CHOP are used as UPR markers for ERS under pathological conditions. BiP is sequestered by binding to unfolded or misfolded proteins, leading to the release from IRE1/PERK/ATF6 and activation of ER-stress sensors^[12], and is currently considered a marker of ERS because of its key role in regulation of ERS sensor activation and ERS initiation^[26-27]. CHOP appears to be a crucial proapoptotic factor found at the convergence point in the regulatory network used to initiate apoptosis caused by persistent ERS^[28-30]. Therefore, in this study, the expression of BiP and CHOP in silica-treated RAW264.7 cells was studied. We found that silica upregulated the mRNA and protein levels of BiP and CHOP. These results suggest that silica treatment induced ERS in RAW264.7 cells.

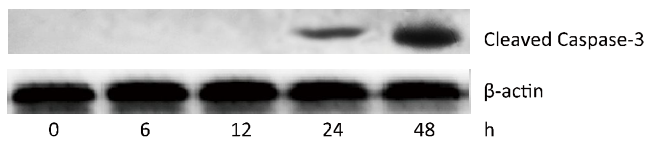


Figure 3. Silica treatment induced expression of caspase-3 in RAW264.7 cells. Cells were treated with silica (200 μ g/mL) for 0, 6, 12, 24, and 48 h. The expression of cleaved caspase-3 was determined by Western blotting.

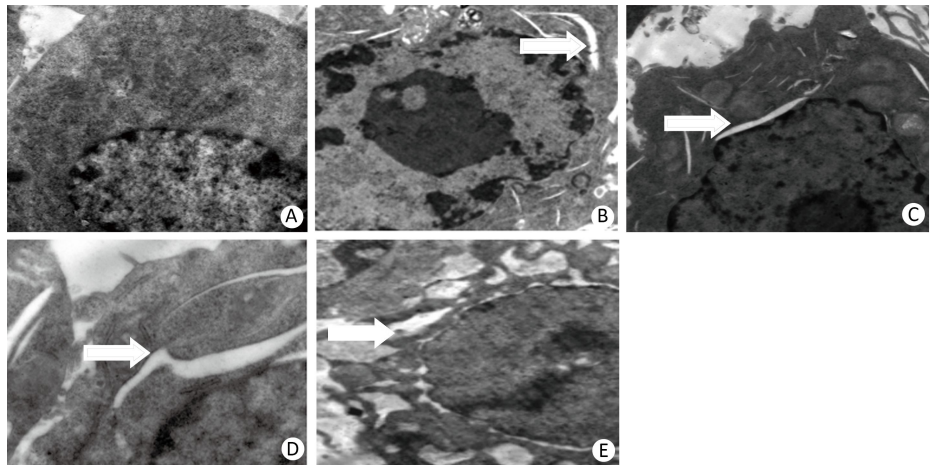


Figure 4. Silica treatment induced endoplasmic reticulum expansion of RAW264.7 cells. Cells were treated with silica (200 μ g/mL) for 0 h (A), 6 h (B), 12 h (C), 24 h (D), and 48 h (E). Morphological changes of the endoplasmic reticulum were observed by transmission electron microscopy (magnification $\times 10,000$). White arrows show expanded endoplasmic reticulum.

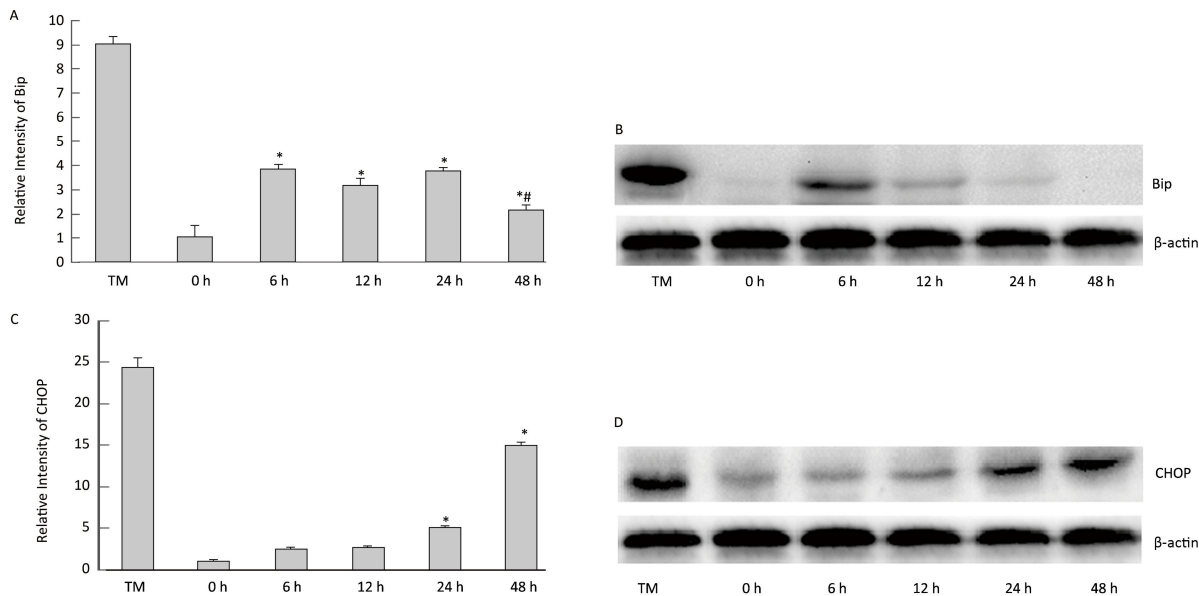


Figure 5. Silica treatment induced endoplasmic reticulum stress of RAW264.7 cells. Cells were treated with silica (200 μ g/mL) for 0, 6, 12, 24, and 48 h. The expression of BiP and CHOP mRNA was determined by real-time PCR (A, C); $^*P < 0.05$, compared with 0 h group, $^{\#}P < 0.05$, compared with 24 h group. The expression of BiP and CHOP proteins was determined by Western blotting (B, D).

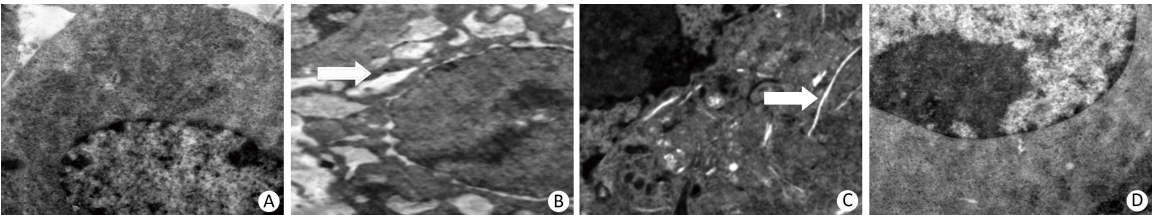


Figure 6. 4-PBA inhibited silica-induced endoplasmic reticulum expansion of RAW264.7 cells. Cells were pre-incubated with 20 $\mu\text{mol/L}$ 4-PBA for 1 h and then stimulated with silica (200 $\mu\text{g/mL}$) for 48 h. Morphological changes of the endoplasmic reticulum were observed by transmission electron microscopy (magnification $\times 10,000$). White arrows show expanded endoplasmic reticulum. (A) without silica and 4-PBA group, (B) silica group, (C) silica and 4-PBA group, (D) 4-PBA group.

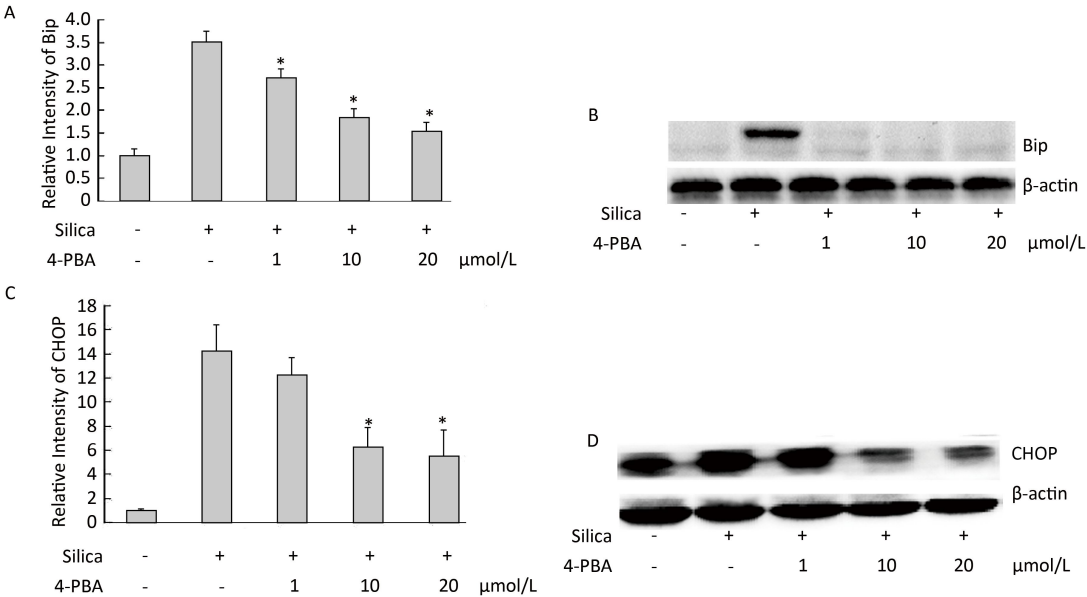


Figure 7. 4-PBA inhibited silica-induced ERS of RAW264.7 cells. Cells were pre-incubated with 1, 10, and 20 $\mu\text{mol/L}$ 4-PBA for 1 h and then stimulated with silica (200 $\mu\text{g/mL}$) for the indicated times. Expression of Bip and CHOP mRNA was determined by real-time PCR (A, C); Expression of Bip and CHOP proteins was determined by Western blotting (B, D). *: $P < 0.05$, compared with silica-stimulated group.

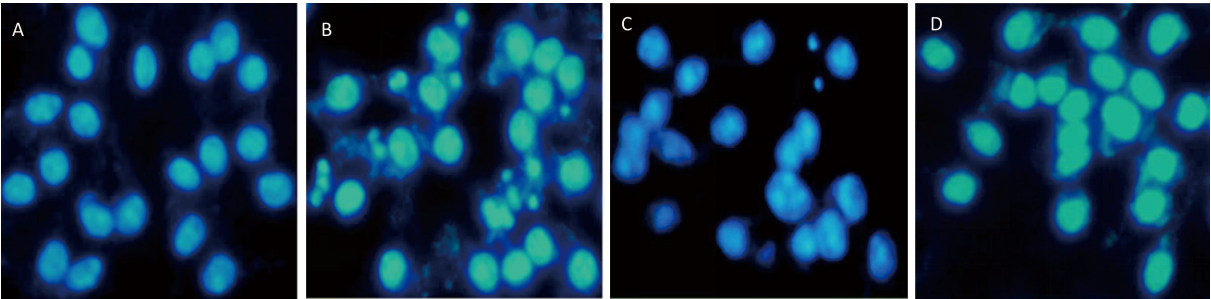


Figure 8. 4-PBA attenuated nuclear condensation in silica-stimulated RAW264.7 cells. Cells were pre-incubated with or without 10 $\mu\text{mol/L}$ 4-PBA for 1 h and then stimulated with or without silica (200 $\mu\text{g/mL}$) for 48 h. Morphological changes of cell nuclei were observed by DAPI staining under a fluorescence microscope (magnification $\times 400$). (A) without silica and 4-PBA group, (B) silica group, (C) silica and 4-PBA group, (D) 4-PBA group.

4-PBA is commonly used to alleviate ER stress and strongly inhibits activation of the IRE1 and ATF6 pathways and downstream pathogenic targets, including nuclear factor- κ B and Akt in ERS-exposed cells^[13]. 4-BPA can interact with hydrophobic domains of misfolded proteins and prevent their aggregation, providing the opportunity for the protein to fold into the proper conformation^[31-32]. We used 4-PBA as an ERS inhibitor to investigate the

correlation between ERS and apoptosis in RAW264.7 cells induced by silica. We found that 4-PBA inhibited silica-induced endoplasmic reticulum expansion and BiP and CHOP expression in RAW264.7 cells. Moreover, 4-PBA attenuated nuclear condensation, reduced apoptotic cells, and decreased the expression of activated caspase-3 in silica- stimulated cells. In addition, following pretreatment with 4-PBA, the viability of silica- stimulated cells increased (data not

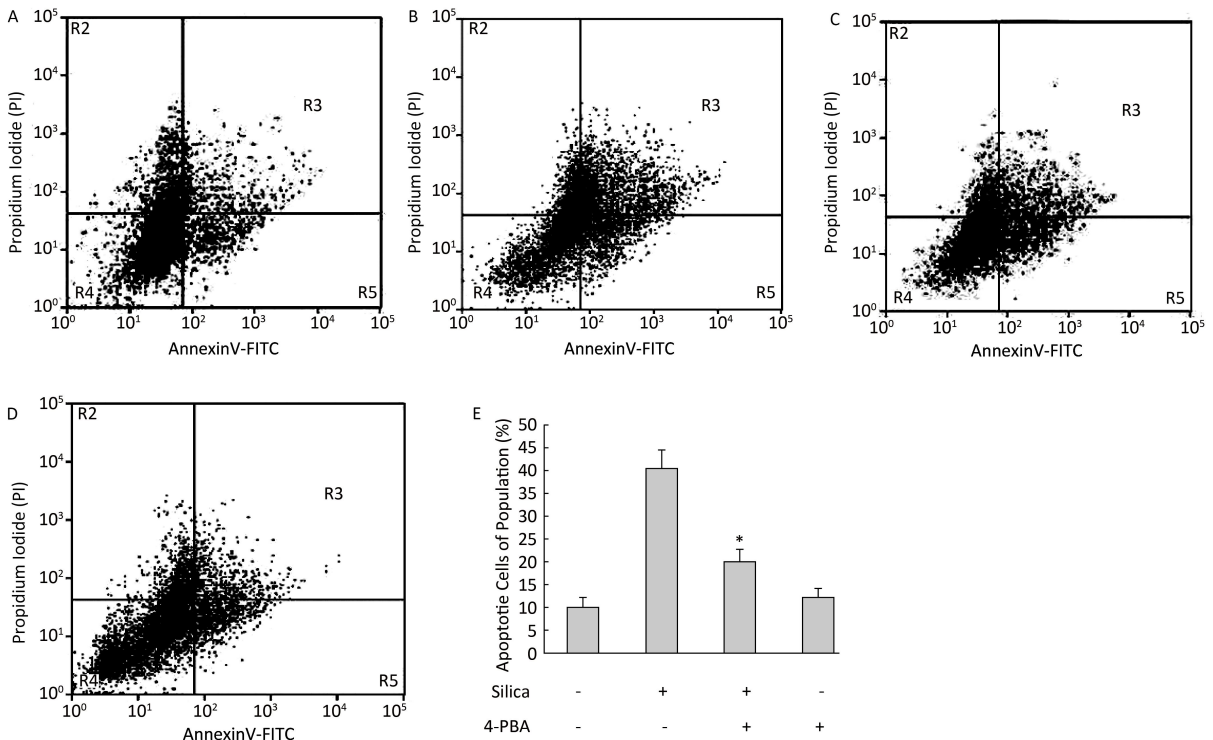


Figure 9. 4-PBA inhibited silica-induced apoptosis of RAW264.7 cells. Cells were pre-incubated with or without 10 μ mol/L 4-PBA for 1 h and then stimulated with or without silica (200 μ g/mL) for 48 h. Apoptotic cells were observed by flow cytometry. (A) without silica and 4-PBA group, (B) silica group, (C) silica and 4-PBA group, (D) 4-PBA group, (E) all histograms show the apoptotic cell populations (%), *: $P < 0.05$, compared with silica-stimulated group.

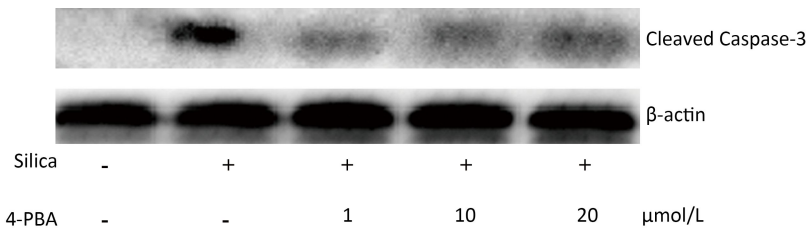


Figure 10. 4-PBA inhibited silica-induced cleaved caspase-3 expression of RAW264.7 cells. Cells were pre-incubated with 1, 10, and 20 μ mol/L 4-PBA for 1 h and then stimulated with silica (200 μ g/mL) for 48 h. Expression of caspase-3 was determined by Western blotting.

shown). Thus, ERS may regulate silica-induced apoptosis in RAW264.7 cells.

This is an advanced study to show that ERS plays an important role in silica-induced apoptosis in AM. These findings provide insight into the molecular mechanisms involved in silica-induced pulmonary disease and the understanding and possible prevention of silicosis.

ACKNOWLEDGEMENTS

We are most grateful to the reviewers for their valuable comments and suggestions for this paper. We would like to extend our sincere thanks to all colleagues and participates involved in this work.

CONFLICT OF INTEREST

The authors have no conflicts of interest to declare.

Received: December 2, 2016;

Accepted: June 2, 2017

REFERENCES

1. Beamer GL, Seaver BP, Jessop F, et al. Acute exposure to crystalline silica reduces macrophage activation in response to bacterial lipoproteins. *Front Immunol*, 2016; 7, 49.

2. Joshi GN, Knecht DA. Silica phagocytosis causes apoptosis and necrosis by different temporal and molecular pathways in alveolar macrophages. *Apoptosis*, 2013; 18, 271-85.

3. Liu H, Cheng Y, Yang J, et al. BBC3 in macrophages promoted pulmonary fibrosis development through inducing autophagy during silicosis. *Cell Death Dis*, 2017; 8, e2657.

4. Liu H, Fang S, Wang W, et al. Macrophage-derived MCP1 mediates silica-induced pulmonary fibrosis *via* autophagy. *Part Fibre Toxicol*, 2016; 13, 55.

5. Jessop F, Hamilton RF, Rhoderick JF, et al. Autophagy deficiency in macrophages enhances NLRP3 inflammasome activity and chronic lung disease following silica exposure. *Toxicol Appl Pharmacol*, 2016; 309, 101-10.

6. Joshi GN1, Knecht DA. Silica phagocytosis causes apoptosis and necrosis by different temporal and molecular pathways in alveolar macrophages. *Apoptosis*, 2013; 18, 271-85.

7. Wang X, Zhang Y, Zhang W, et al. MCP1P1 regulates alveolar macrophage apoptosis and pulmonary fibroblast activation after *in vitro* exposure to silica. *Toxicol Sci*, 2016; 151, 126-38.

8. Yao SQ, Rojanasakul LW, Chen ZY, et al. Fas/FasL pathway-mediated alveolar macrophage apoptosis involved in human silicosis. *Apoptosis*, 2011; 16, 1195-204.

9. Chen S, Yuan J, Yao S, Jin Y, et al. Lipopolysaccharides may aggravate apoptosis through accumulation of autophagosomes in alveolar macrophages of human silicosis. *Autophagy*, 2015;

11, 2346-57.

10. Wang L, Scabilloni JF, Antonini JM, et al. Induction of secondary apoptosis, inflammation and lung fibrosis after intratracheal instillation of apoptotic cells in rats. *Am J Physiol Lung Cell Mol Physiol*, 2006; 290, L695-L702.

11. Wu J, Kaufman RJ. From acute ER stress to physiological roles of the unfolded protein response. *Cell Death Differ*, 2006; 13, 374-84.

12. Bertolotti A, Zhang Y, Hendershot LM, et al. Dynamic interaction of BiP and ER stress transducers in the unfolded-protein response. *Nat Cell Biol*, 2000; 2, 326-32.

13. Zhang K, Kaufman RJ. From endoplasmic-reticulum stress to the inflammatory response. *Nature*, 2008; 454, 455-62.

14. Su J, Zhou L, Kong X, et al. Endoplasmic reticulum is at the crossroads of autophagy, inflammation, and apoptosis signaling pathways and participates in the pathogenesis of diabetes mellitus. *J Diabetes Res*, 2013; 2013, 193461.

15. Sano R, Reed JC. ER stress-induced cell death mechanisms. *Biochim Biophys Acta*, 2013; 1833, 3460-70.

16. Le Pape S, Dimitrova E, Hannaert P, et al. Polynomial algebra reveals diverging roles of the unfolded protein response in endothelial cells during ischemia-reperfusion injury. *FEBS Lett*, 2014; 588, 3062-7.

17. Zheng XY, Xu J, Chen XI, et al. Attenuation of oxygen fluctuation-induced endoplasmic reticulum stress in human lens epithelial cells. *Exp Ther Med*, 2015; 10, 1883-7.

18. Krebs J, Agellon LB, Michalak M. Ca(2+) homeostasis and endoplasmic reticulum (ER) stress: An integrated view of calcium signaling. *Biochem Biophys Res Commun*, 2015; 460, 114-21.

19. Hu YB, Lin Z, Feng DY, et al. Silica induces alarminogen activator inhibitor-1 expression through a MAPKs/AP-1-dependent mechanism in human lung epithelial cells. *Toxicol Mech Methods*, 2008; 18, 561-7.

20. Geiser M. Update on macrophage clearance of inhaled micro- and nanoparticles. *J Aerosol Med Pulm Drug Deliv*, 2010; 23, 207-17.

21. Beamer CA, Migliaccio CT, Jessop F, et al. Innate immune processes are sufficient for driving silicosis in mice. *J Leukoc Biol*, 2010; 88, 547-57.

22. Johansson AC, Appelqvist H, Nilsson C, et al. Regulation of apoptosis-associated lysosomal membrane permeabilization. *Apoptosis*, 2010; 15, 527-40.

23. Li X1, Hu Y, Jin Z, et al. Silica-induced TNF-alpha and TGF-beta1 expression in RAW264.7 cells are dependent on Src-ERK/AP-1 pathways. *Toxicol Mech Methods*, 2009; 19, 51-8.

24. Laing S, Wang G, Briazova T, et al. Airborne particulate matter selectively activates endoplasmic reticulum stress response in the lung and liver tissue. *Am J Physiol Cell Physiol*, 2010; 299, 736-49.

25. Yun-Ji Lim, Ji-Ae Choi, Hong-Hee Choi, et al. Endoplasmic reticulum stress pathway-mediated apoptosis in macrophages contributes to the survival of mycobacterium tuberculosis. *PLoS One*, 2011; 6, e28531.

- 26.Chistiakov DA, Sobenin IA, Orekhov AN, et al. Role of endoplasmic reticulum stress in atherosclerosis and diabetic macrovascular. *Biomed Res Int*, 2014; 2014, 610140.
- 27.Hotamisligil GS. Endoplasmic reticulum stress and the inflammatory basis of metabolic disease. *Cell*, 2010; 140, 900-17.
- 28.Makareeva E, Avilis NA, Leikin S, et al. Chaperoning osteogenesis: new protein-folding-disease aradigms. *Trends Cell Biol*, 2011; 21, 168-76.
- 29.Chiribau CB, Gaccioli F, Huang CC, et al. Molecular symbiosis of CHOP and C/EBP β Isoform LIP contributes to endoplasmic reticulum stress-induced apoptosis. *Mol Cell Biol*, 2010; 30, 3722-31.
- 30.Teske BF, Fusakio ME, Zhou D, et al. CHOP induces activating transcription factor 5 (ATF5) to trigger apoptosis in response to perturbations in protein homeostasis. *Mol Biol Cell*, 2013, 24, 2477-90.
- 31.Ben Mosban, Alfany I, Martel C, et al. Endoplasmic reticulum stress inhibition protects steatotic and non-steatotic livers in partial hepatectomy under ischemia-reperfusion. *Cell Death Dis*, 2010; 1, e52.
- 32.Rachel EC, Elise B, Kaitlyn EW, et al. 4-Phenylbutyrate inhibits tunicamycin-induced acute kidney injury *via* CHOP/GADD153 repression. *PLos One*, 2014; 9, e84663.